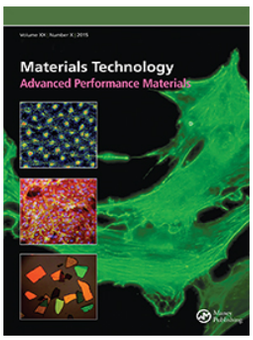

Taylor & Francis
Taylor & Francis Group

Materials Technology
Advanced Performance Materials

ISSN: 1066-7857 (Print) 1753-5557 (Online) Journal homepage: https://www.tandfonline.com/loi/ymte20

Advanced 3Y-TZP bioceramic doped with Al_2O_3 and CeO_2 potentially for biomedical implant applications

Mohsen Golieskardi, Meenaloshini Satgunam, Dinesh Ragurajan, Md Enamul Hoque, Angela Min Hwei Ng & Lohashenpahan Shanmuganantha

To cite this article: Mohsen Golieskardi, Meenaloshini Satgunam, Dinesh Ragurajan, Md Enamul Hoque, Angela Min Hwei Ng & Lohashenpahan Shanmuganantha (2019): Advanced 3Y-TZP bioceramic doped with Al_2O_3 and CeO_2 potentially for biomedical implant applications, Materials Technology

To link to this article: https://doi.org/10.1080/10667857.2019.1578912

Published online: 20 Feb 2019.

MATERIALS TECHNOLOGY
https://doi.org/10.1080/10667857.2019.1578912

Taylor & Francis
Taylor & Francis Group

Advanced 3Y-TZP bioceramic doped with Al_2O_3 and CeO_2 potentially for biomedical implant applications

Mohsen Golieskardi[a], Meenaloshini Satgunam[a], Dinesh Ragurajan[a], Md Enamul Hoque[b], Angela Min Hwei Ng[c] and Lohashenpahan Shanmuganantha[c]

[a]Department of Mechanical Engineering, College of Engineering, Universiti Tenaga Nasional, Kajang, Malaysia; [b]Department of Biomedical Engineering, Military Institute of Science and Technology (MIST), Dhaka, Bangladesh; [c]Tissue Engineering Center, Universiti Kebangsaan Malaysia Medical Center, Kuala Lumpur, Malaysia

ABSTRACT

This research studies 3 mol% yttria-stabilized zirconia (3Y-TZP) investigating the effects of Al_2O_3 and CeO_2 dopants on the stability of tetragonal phase and the microstructure of 3Y-TZP determined over the operating temperature ranging from 1250°C to 1550°C. It is found that the mechanical properties of 3Y-TZP are dependent on the sintering temperature and the dopant amount. The current study reveals that the optimum sintering temperature is 1450°C for all 3Y-TZP samples while attaining more than 98% of the theoretical density (6.1g/cm^3). With optimum dopants, the 3Y-TZP ceramic samples demonstrate the Vickers hardness of 10.9 GPa and fracture toughness (K_{IC}) of 10 MPa.m$^{1/2}$. Fracture toughness increases with the dopant content, indicating that the annihilation of oxygen vacancies in 3Y-TZP is responsible for the instability of the t-ZrO_2 lattice. To investigate the biocompatibility of 3Y-TZP, cell culture study was performed using osteoblast cells. The results demonstrate a high percentage of cell attachment and proliferation that confirmed the biocompatibility of synthesized 3Y-TZP.

ARTICLE HISTORY
Received 3 October 2018
Accepted 21 January 2019

KEYWORDS
Bioceramic; 3Y-TZP; cell morphology; cell proliferation; cytotoxicity; mechanical properties

Introduction

Biomaterials are implanted in human bodies to replace damaged/diseased tissues. As for the developments in implantology field, many materials have been invented to improve prostheses quality applied for either fixing or replacing the body tissues. Since most of the biomaterials used for this purpose are ceramics, metals and polymers, spectacular improvements have occurred in many cases such as bone reconstruction, and replacing joints or teeth. The overall innovations on both surface properties and bulk modifications in this regards are enormous. When prosthesis is placed within the body, it interacts with the living organs. Therefore, it is important that the material should be biocompatible, e.g. a successful implant provides enough material tolerance to support a higher biocompatibility grade. A biomaterial can be produced from various sources such as metal, polymer or ceramic, depending on its functionality [1–5]. There are advantages and limitations associated with each material category. For example, ceramic is well-known for its biocompatibility. However, it is frequently characterized by its high hardness and low resistance to fracture. On the other hand, bioceramics such as 3 mol% yttria-stabilized zirconia (3Y-TZP), porcelain are often used in dental applications due to their biocompatibility and promising mechanical properties [6–8]. More importantly, very fine grain microstructures may be obtained (particle size ~0.5 μm) from Y-TZP powders. The fracture toughness, hardness and fracture strength of 3Y-TZP are 4–8 MPa.m$^{1/2}$, 10–12 GPa and 900–1200 MPa, respectively [9], which are relatively high as compared to those of other bioceramics [10]. The superior fracture toughness exhibited by Y-TZP ceramics are due to the transformation toughening mechanism, which involves spontaneous phase transformation from tetragonal (t) to monoclinic (m) zirconia occurring as a crack propagates through the material, a mechanism known as transformation toughening [11].

However, one of the major limitations of Y-TZP ceramics as engineering materials is the undesirable surface-initiated phase transformation from the (t) to (m) symmetry accompanied by property degradation during exposure in humid atmosphere (water and steam) at temperatures ranging from 20°C to 500°C. Besides, ceramic can undergo a slow, tetragonal to monoclinic phase transformation at the samples surface in a humid atmosphere followed by microcracking and a serious loss in strength, a phenomenon subsequently known as ageing or low-temperature degradation (LTD) [12–14].

To overcome LTD in Y-TZP, inclusion of sintering additives such as TiO_2, SiO_2, Al_2O_3, MgO, CeO_2, etc. have been investigated by many researchers since this is the most effective and simplest way to achieve a dense body at low-temperature sintering, thus helps to

CONTACT Mohsen Golieskardi Mohsen_golieskardi@yahoo.com Department of Mechanical Engineering, College of Engineering, Universiti Tenaga Nasional, 43000 Kajang, Malaysia

improve the mechanical properties of the sintered material [15–20]. Samodurova [21] reported that combined effect of alumina and silica (up to 0.25 wt%) co-doping to 3Y-TZP results in improved resistance to ageing without affecting the mechanical properties. Small addition of Al_2O_3 (<5%) is able to promote densification of Y-TZP ceramic. It is observed that small addition of Al_2O_3 could enhance sintering at low temperatures and cause impressive grain growth at higher sintering temperatures.

Microstructure of the ceramics can be altered, leading to dispersion strengthening through various mechanisms [22–24] that eventually enhances the mechanical property of the material. The effects of Al_2O_3 and 3Y-TZP ceramic composites in vivo environment have been studied by Santos et al. [25]. This analysis showed promising results, because the viability of 90% of the composite material was clearly above the 80% viability limit, which indicates an excellent biocompatibility of the material. Therefore, it can be affirmed that the 3Y-TZP–Al_2O_3 composite material can be classified as non-cytotoxic and therefore having great potential for possible applications as implants. Another attractive dopant for the stabilization of 3Y-TZP is cerium oxide. It has been reported that the minor addition of cerium oxide (up to 0.5 wt %) to 3Y-TZP results in improved resistance to ageing without affecting the mechanical properties. Rejab et al. [26] indicated that through increasing CeO_2 content the bulk density was increased and the percentage of porosity was decreased. This can improve the toughness of the materials.

The aim of this work is to study the influence of the combined effects of aluminium oxide and cerium oxide co-doping on the densification, Vickers hardness, fracture toughness and cytotoxicity of 3 mol% yttria-stabilized zirconia materials commonly utilized in the implants.

Experimental procedures

Synthesis of 3Y-TZP ceramic and preparation of test samples

The starting materials used were as-received commercial 3 mol% Y-TZP (Kyoritsu, Japan) cerium oxide and aluminium oxide powders of 99.9% purity (Sigma Aldrich). The 3 mol% Y-TZP powder was combined with various percentages of aluminium oxide and cerium oxide powders; i.e. undoped, 0.3wt% and 0.5wt% using a wet-milling method. The raw materials were weighed in appropriate quantities, ball milled in ethanol using zirconia balls as the milling media. The resulting slurry was oven dried and sieved to obtain micro-scale ready-to-press powder. Samples were pressed accordingly into discs (20 mm diameter) and bars (4mmx 13mmx32mm) and underwent cold-isostatic pressing at 200 MPa before being sintered at various temperatures (1250°C –1550°C), with a ramp rate of 10°C/min and holding time of 2 h.

Physical and mechanical characterizations

The bulk densities of samples were determined using the Archimedes method (Mettler-Toledo AG204). Firstly, the samples were polished before their Vickers hardness (Hv) values were measured using micro-indentation. During the test, a load of 1 kg was exerted using a pyramidal jewel indenter for 10 s. Ten measurements were performed on each sample. On the other hand, the K_{IC} values of all samples were determined by measuring the cracks created upon exerting a load of 2 kg for 10 s. The crack was analyzed by using an image analysis program. Here, the equation proposed by Niihara et al. was employed [27]. The measurement was repeated 10 times for each sample.

Cell culture study

$2x10^5$ cultured human osteoblasts (Passage 3 or 4) were seeded onto each Al_2O_3/CeO_2 (either with the ratio of 0.3/0.3 or 0.3/0.5) disc placed in a 24 well plate. After 24 h, seeded discs were shifted to a new 24-well plate. At day 1, day 4 and day 7, the seeded discs were transferred to a new plate. At the respective time points, 40ul of PrestoBlue™ Reagent (Invitrogen, USA) was added directly into the well with 360ul of culture medium containing the seeded discs. The seeded disc samples placed into the well-plate were incubated for 2 h at 37°C. After incubation, the well-plate was shaken mildly for more uniform distribution of seeded cells into the disc samples, and transferred 100ul of the reaction mix (in triplicates) into a 96-well plate. Absorbance was read at 570nm with a reference wavelength of 600nm using a microplate reader (BioTek, USA). Living cells that are metabolically active will reduce the non-fluorescent dye resazurin to a strongly fluorescent dye resorufin. Absorbance is proportional to the number of viable cells. Seeded discs after the Presto Blue assay at Day 7, were subsequently incubated in culture media twice for 24 h at 37°C in CO_2 incubator. After 24 h, the seeded discs were rinsed with Dubellco's phosphate-buffered solution (DPBS) for 5 min and incubated with pre-warmed LIVE/DEAD assay reagents for 30–45 min at room temperature. Following incubation, the seeded discs were rinsed with DPBS and viewed under the confocal laser scanning microscope (Nikon A1, Nikon, Japan).

Qualitative observation of live/dead cell

Seeded discs after the Presto Blue assay at Day 7 were incubated in a culture media. The incubation was performed twice in a CO_2 incubator operating at 37°C. After 1 day, the seeded discs were rinsed in the Dubellco's Phosphate-Buffered Solution (DPBS) for 5 min. Subsequently, the discs were incubated at room temperature with the pre-warmed LIVE/DEAD assay reagents for 30–45 min. After that, the seeded discs were rinsed with DPBS and viewed under the confocal laser scanning microscope (Nikon A1, Nikon, Japan). Indeed, the cell viability depends on its physical and biochemical characteristics. Frequent intracellular esterase activity and enzymatic conversion of the nonfluorescent cell-permeant calcein AM to the fluorescent calcein are common in a live cell. Also, green fluorescence is produced intensively in a live cell (ex/em ~495 nm/~515 nm) due to the ubiquitous polyanionic dye calcein. By magnifying the dying/dead cells using 40x enhancement of fluorescence (upon attaching the cells to the nucleic acids), EthD-1 accesses the damaged membranes of these cells by examining the bright red fluorescence formed (ex/em ~495 nm/~635 nm). EthD-1 is not considered in live cells. Table 1 reports the quality of cell attachment and the grade of cell viability on the disc.

Cell morphology and cell-material interphase

Cell-seeded constructs were immediately fixed in 4% cold glutaraldehyde in phosphate buffer, pH 7.5, stored at 4°C, and then rinsed 3 times with PBS and dehydrated in a graded ethanol series. The samples were then post-fixed with 1% osmium tetraoxide for 2 h at 4°C and dehydrated with increasing concentration of acetone (35%, 50%, 75%, and 95% for 10 min each and three changes in 100% for 15 min). The dehydrated samples were transferred into specimen basket and immersed in 100% acetone, and dried with critical point dryer (Baltec 030 CPD, Liechtenstein, Switzerland) for approximately 30 min. Thereafter, the samples were mounted on copper stub using double-sided carbon tape and sputter coated (Polaron E5100 sputter coater, Milan, Italy) with gold–palladium. The samples were then examined using Phenom G2 Pro Desktop scanning electron microscope (Phenom-World, Netherlands).

Table 1. Grading for cell attachment on the material.

Quality of cell attachment	Description
High	All most the entire area are covered with cells
Moderate	Much area covered with cells
Low	Little area covered with cells
Nil	No cell attachment can be observed

Results and discussions

Bulk density

The variation of bulk density for 3Y-TZP with different amounts of Al_2O_3 and CeO_2 sintered between 1250°C and 1550°C is presented in Figure 1. The result shows that both compositions exhibited a common densification trend. The 0.3wt% CeO_2/0.3wt% Al_2O_3-3Y-TZP composition achieved considerably higher values of approximately 97.5% (5.956 g/cm^3) of the theoretical density (6.1 g/cm^3) when sintered at 1450°C as compared to density achieved for the undoped ceramic 94% (5.88 g/cm^3).

Vickers hardness

The influence of sintering temperature and inclusion of CeO_2 and Al_2O_3 on the Vickers hardness of 3Y-TZP is demonstrated in Figure 1. It was observed that the hardness of doped 3Y-TZPs showed a trend similar to the bulk density in Figure 2. The results obtained confirmed that the addition of CeO_2 and Al_2O_3 enhanced the hardness of 3Y-TZP when sintered at 1450°C. The hardness was found to be the lowest (~7 GPa) when sintered at 1250°C and increased to ~8.4 GPa at the sintering temperature of 1350°C before reaching the maximum value of ~9.8 GPa at the sintering temperature of 1450°C.

Besides that, the hardness values of all the CeO_2 and Al_2O_3 doped specimens was observed to be higher than that of the undoped material when sintered between 1250°C and 1550°C. The hardness value trend of the 0.3wt% Al_2O_3/0.3wt% CeO_2 and 0.3wt% Al_2O_3/0.5wt% CeO_2 doped specimens was almost similar, i.e. increasing rapidly from ~9.7 GPa to ~9.4 GPa, when sintered at 1250°C to the values of more than 10.7 GPa and 10.9 GPa at 1450°C, respectively.

Fracture toughness

The variation of fracture toughness for Al_2O_3 and CeO_2 doped 3Y-TZP against sintering temperature is shown in Figure 3. The results indicated that both compositions appeared to have negligible effect on the fracture toughness of 3Y-TZP at temperatures from 1250°C to 1350°C. The fracture toughness values were found to be between 4 MPam$^{1/2}$ and 6 MPam$^{1/2}$. The phenomenon that the fracture toughness (K_{IC}) value did not vary significantly with sintering temperature indicated that the additions of CeO_2 and Al_2O_3 below 1350°C did not affect the resistance of 3Y-TZP in propagating crack. However, when sintered above 1350°C, the K_{IC} of the doped compositions started to increase with increasing temperature; e.g. 0.3wt% Al_2O_3 and 0.5wt% CeO_2-doped 3Y-TZP and 0.3wt% Al_2O_3 and 0.3wt% CeO_2-doped 3Y-TZP exhibiting a significant increase from 5.2 MPa.m$^{1/2}$ to 9 MPa.m$^{1/2}$ and 4.7 MPa.m$^{1/2}$ to 10 MPa.m$^{1/2}$, respectively.

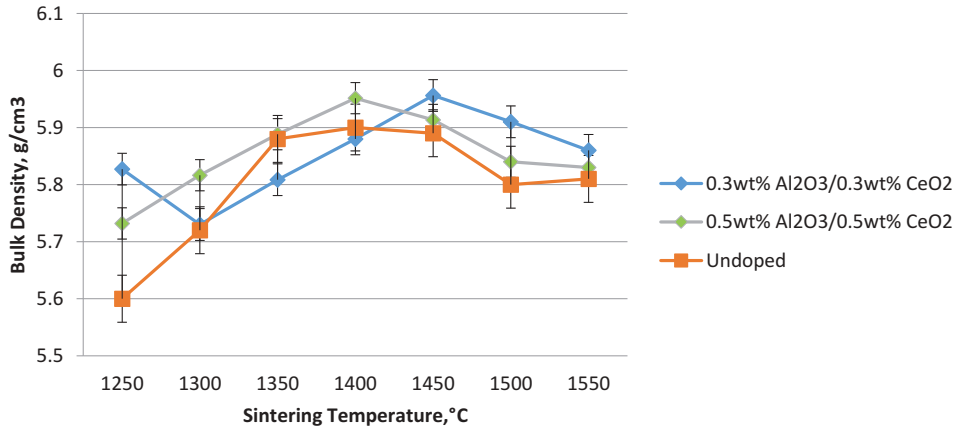

Figure 1. Effect of CeO_2 and Al_2O_3 additions on the bulk density of 3Y-TZP sintered between 1250–1550°C.

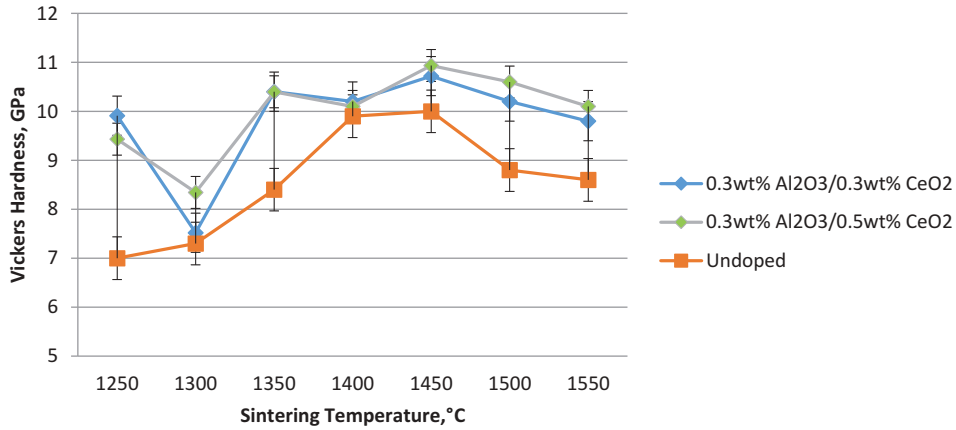

Figure 2. Effect of CeO_2 and Al_2O_3 additions on the Vickers hardness of 3Y-TZP sintered from 1250°C to 1550°C.

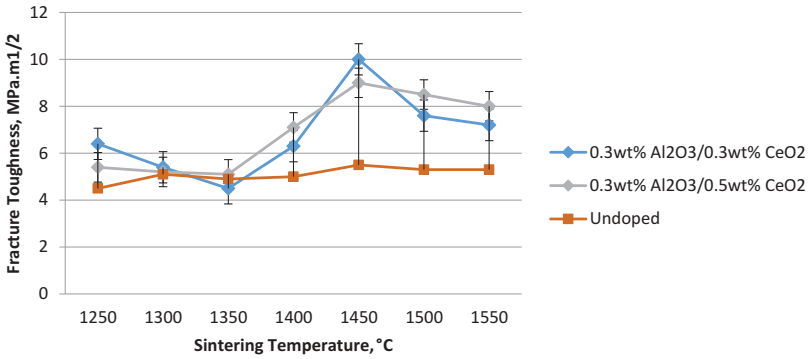

Figure 3. Influence of dopant additions and sintering temperature on the fracture toughness of 3Y-TZP.

Cell viability and proliferation assay (quantitative)

Cell proliferation of human osteoblasts grown on 3Y-TZP surfaces at days 1, 4 and 7 is presented in Figure 4. There was no change in cell culture at each culture time. The MTT assay showed no significant differences among the samples at days 1 and 4, supporting the epifluorescence images of cultures. Additionally, cells adhered better to culture plastic dish (control sample) compared to both compositions.

Cell leachate study

Figure 5(a-c) shows the cell numbers of $0.3Al_2O_3$ /$0.3CeO_2$ and $0.3Al_2O_3/0.5CeO_2$ doped-3Y-TZP samples over leachate exposure time. At Day 1, the material containing $0.3Al_2O_3/0.5CeO_2$ showed greater viability than its counterpart as there was an increase in cell amount in compared to the control specimen. Eventually, there was a 10% increase in cell proliferation by the end of Week 1. The other values are shown in Table 2. At the end of day 4, it was observed that the cell had proliferated by 8%, and at the end of day 7, the cells proliferated by 1.5%. Though

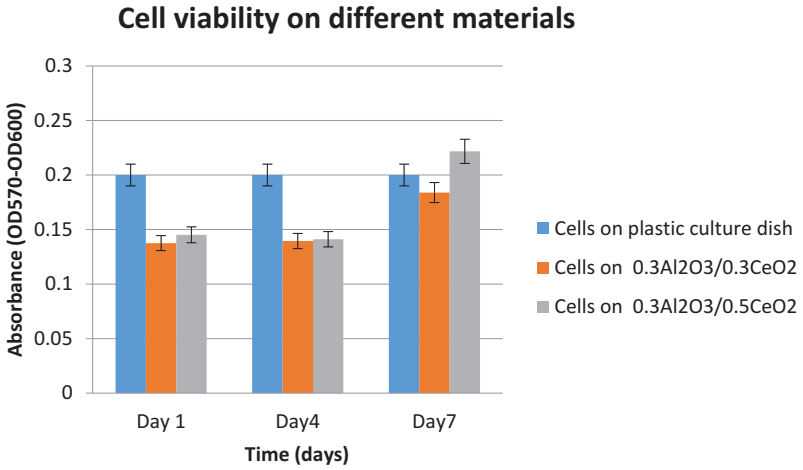

Figure 4. Cell viability (absorbance reading) on Al_2O_3 and CeO_2 discs vs plastic culture dishes.

Table 2. Percentage difference from negative control for each material specimen (week 4 only).

Day	Percentage deviation from control(0.3:0.3)	Percentage deviation from control(0.3:0.5)
1	−8%	+10%
4	−2%	+8%
7	−11%	+1.5%

there was a decrease in proliferation rate as compared to day 1, the specimen still indicated a positive proliferation rate as compared to the control specimens.

As for the 0.3wt% Al_2O_3/0.3wt% CeO_2 material, it was seeded with 20,000 cells during initial testing and the cells rapidly multiplied to approximately 48,000 cells. However, at the end of day 1, a slight decrease in the amount of cells (8%) was detected. At day 4, a decrease of 2% of cells were reported and finally at day 7, a decrease of (11%) of cells were reported. Although at the end of day 7 a consistent decrease in cell proliferation was reported. However, this value was above the control sample which still indicates the samples 0.3wt% Al_2O_3/0.3wt% CeO_2 material is not toxic.

Live-dead detection of cells (qualitative imaging)

Images of the stained seeded disc under the confocal laser scanning microscope were captured using a high-resolution CCD camera as shown in Figures 6 and 7. The features of cell attachment and cell viability on the discs viewed under the fluorescent microscope. It was found that the sample containing 0.3wt% Al_2O_3/0.5wt% CeO_2 seemed to be more variable in terms of percentage of cell attachment and cell viability. In general, both materials showed a high percentage of cell attachment and moderate cell viability.

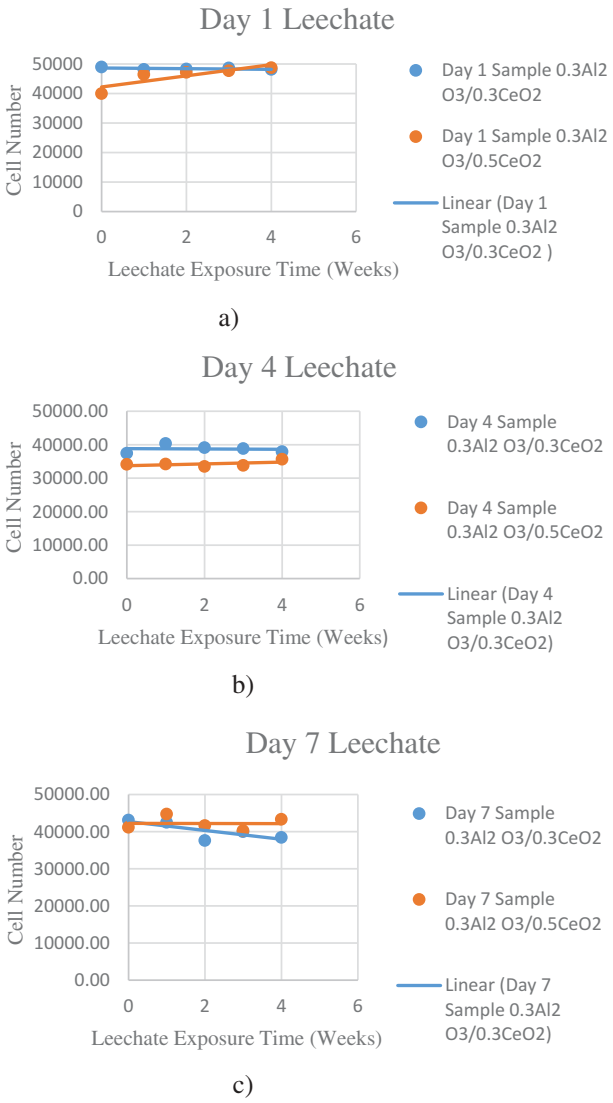

Figure 5. The comparison of cell number versus cell leachate for samples containing 0.3wt% Al_2O_3/0.3wt% CeO_2 and 0.3wt % Al_2O_3/0.5wt% CeO_2 over 7 days.

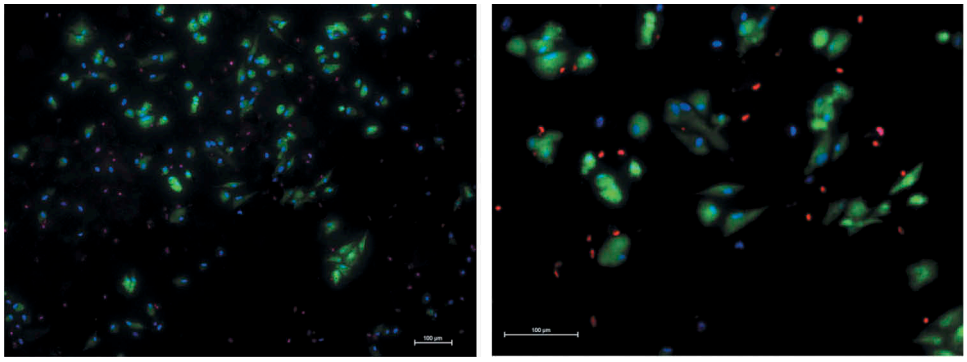

Figure 6. Fluorescent micrographs of cells seeded of 0.3wt% Al_2O_3/0.3wt% CeO_2. (Green cells are live cells Red cells are dead or dying cells).

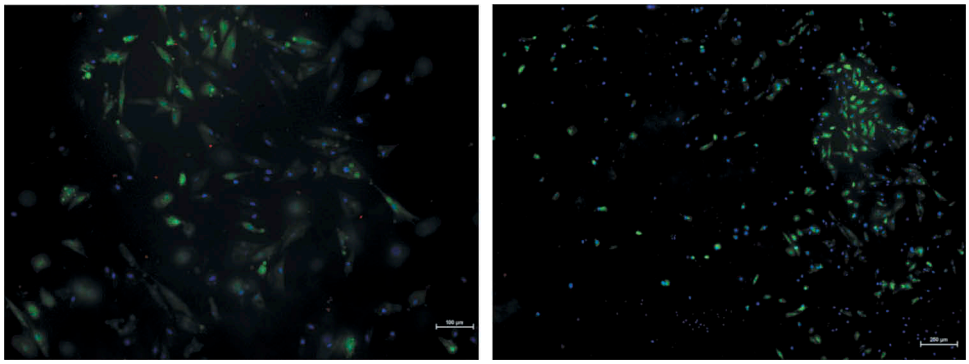

Figure 7. Fluorescent micrographs of cells seeded of 0.3wt% Al_2O_3/0.5wt% CeO_2. (green cells are live cells, red cells are dead or dying cells and blue are nucleus).

Cell morphology and cell-material interphase study

Seeded human osteoblasts appeared to be well attached on the surface of both types of specimens. At day 1, cells appeared to be plump (rounded), similar to young cells and many had developed extensive pseudopodia as shown in Figure 8. At day 3, cells appeared to be slightly more flattened which is likened to a more mature phenotype of osteoblast. At day 7, cells appeared to be even more flattened, with some demonstrating crust-like surface that appeared like mineral deposition. The final grain size and cell shape determined for all specimens are shown in Table 3. No clear distinction could be made between the morphology of cells seeded on either disc type. No cells were seen penetrating into the inner spaces of the material.

Table 3. Summary of the final grain size and cell shape determined for all specimens.

Specimen	Avg. Grain Size(μm)	Shape of Cell
A1	452.04	Plump
B1	390.15	
A2	437.98	Slightly flattened
B2	493.1	
A3	504.42	Slightly flattened
B3	446.2	

Discussion

Physical characterization

The results showed that the addition of Al_2O_3 and CeO_2 dopants had a large effect on the mechanical properties of 3Y-TZP. The densification behaviour of the material in terms of density was studied under various conditions of sintering temperature as well as dopant content. The achievement of a higher density is most likely due to the reduction in porosity through high sintering temperatures. Due to the higher amount of heat energy, there is an increased fusion rate of particles experienced by the material. It is interesting to note that the addition of aluminium oxide and cerium oxide (sintered in between 1350°C and 1450°C) can increase the density of 3Y-TZP by 2–5%. This finding is consistent with previous studies [28,29], where both CeO_2 and Al_2O_3 have been used as sintering additives in Y-TZP. The same additives have been previously used in ceramic matrices as well. By performing sintering at 1400°C for 1 h, Kimura et al. [30] reported that additives such as CuO and MnO_2 (with 0.1wt%-0.5wt% of MnO_2) could improve the bulk density as well. This favourable effect happens at a lower temperature as well that renders the microstructural property of Al_2O_3 highly homogeneous. Beyond 1400°C, density reduction is

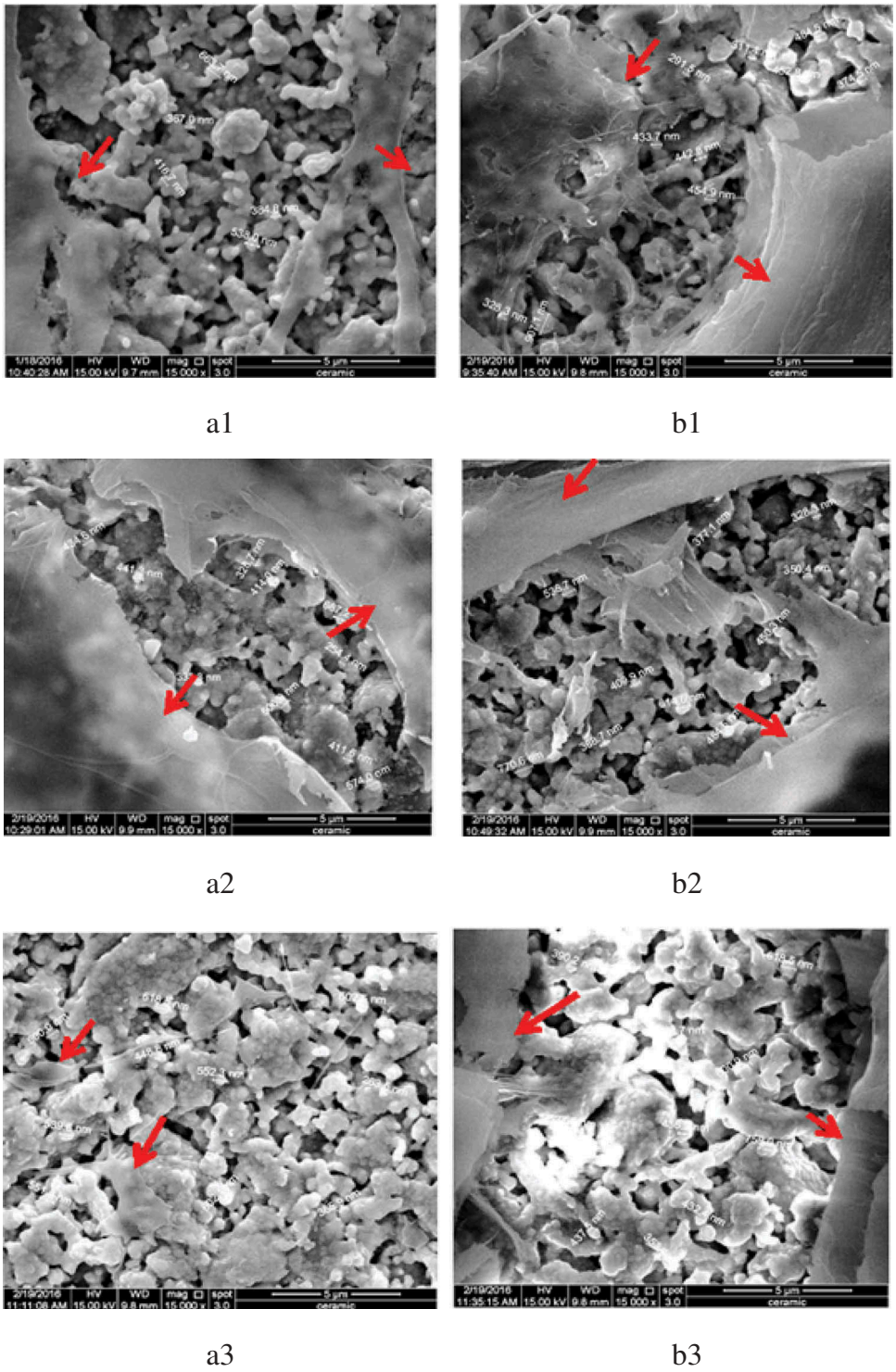

Figure 8. Cell Morphology and Cell-Material Interphase Study for specimens containing at 0.3wt% Al_2O_3/0.3wt% CeO_2 and 0.3wt % Al_2O_3/0.5wt% CeO_2 at day 1(A1 & B1), day 3(A2 & B2) and day 7(A3 & B3) respectively.

observed due to the increase in grain size and intergranular cracking within the samples.

Mechanical characterization

The mechanical properties of the sintered material were evaluated for their hardness and fracture toughness as a function of dopant content as well as sintering temperature which were plotted in Figures 1 and 3, respectively. It is evident that when Al_2O_3 and CeO_2 were added to 3Y-TZP, they resulted in a gradual increase in hardness and fracture toughness, with a relatively high rate of increase at 1450°C. However, it was seen that regardless of dopant additions, the hardness and fracture toughness of all the 3Y-TZPs started to decrease when sintered above 1450°C. This trend of increasing hardness until a maximum at a certain sintering temperature followed by a continuous decline

thereafter with further sintering as seen in the present study is in agreement with the work of Ramesh et al. [31]. Two possible explanations can be made for the decline in hardness of this sample when sintered above 1400°C. Firstly, hardness is strongly dependent on bulk density, which decreased considerably during the temperature range as shown in Figure 2 and secondly, it can be associated with the reduction of tetragonal phase content and an increase in the cubic phase formation in the zirconia matrix with increasing temperature.

The significant increase of K_{IC} in these compositions might be attributed to the transformation toughening effect. The influx of yttria to certain tetragonal grains during sintering tends to tighten the tetragonal grains and lead to excessive grain growth. Subsequently, the yttria-rich cubic phase is formed. Upon cooling (to room temperature), the minority grains suffering from intense yttria dissolution would undergo phase transformation, i.e. from (t) to (m) phase. The tetragonal grains that have undergone slight yttria depletion would become metastable and remain in their tetragonal forms. These metastable grains are likely to undergo transformation toughening (upon indentation) leading to large fracture toughness. The above finding has been supported by Kimura et al. [30].

Assessment of in vitro bioactivity

Upon dopant additions, the bioactivity of 3Y-TZP was analyzed using a few types of test such as cell viability and proliferation assay (Quantitative), cell leachate, live-dead detection (Imaging) and cell morphology and cell-material interphase study (Scanning Electron Microscopic Evaluation). The physical and mechanical properties were taken into account when selecting the samples used for the in vitro study; 3Y-TZP samples containing 0.3wt% Al_2O_3 and 0.5wt% CeO_2 sintered at 1450°C were used because they displayed highest densification behaviour and superior mechanical properties.

Cell viability and proliferation assay

At days 1 and 4, no significant differences in terms of cell morphology were detected between the two compositions; cells exhibited polygonal shapes with long cytoplasmic extensions. A slightly lower cell number on day 4 can be observed for the 0.3wt% Al_2O_3/0.5wt% CeO_2 composition however at day 7; cell multilayering took place for both compositions. The MTT results confirmed a major progression of human osteoblasts cell cultures on the $0.3Al_2O_3$ /$0.5CeO_2$ doped-3Y-TZP surface, as revealed by significantly higher values of 0.22 at day 7 compared to the $0.3Al_2O_3/0.3CeO_2$ surface with absorbance rate of 0.18. Strickstrock et.al [32]. conducted a cell viability test using 3Y-TZP for a period of 7 days. Investigated samples demonstrated high cell viability (>95%) with no signs of cytotoxic effects. Similar results were also reported for fully differentiated primary human osteoblasts. Ardlin et.al [33] also investigated cell viability on various types of 3Y-TZP composition materials discovered that cellular viability showed a significant increase upon immersion of about 2 to 3 days.

Cell leachate

At the end of Week 1, there was 10% increase in cell proliferation on $0.3Al_2O_3/0.5CeO_2$ samples as compared to $0.3Al_2O_3/0.3CeO_2$ samples. It was also found that cell number increased almost two times of the original cell number after day 1 of immersion. A positive value indicates that the cell number exceeds the control and a negative value reflects a reduction in proliferation rate of the cells. The $0.3Al_2O_3/0.3CeO_2$ samples, however, showed a contrast in cell proliferation, as the numbers of cells were seen to have reduced by about 11%. It is evident that the $0.3Al_2O_3/0.5CeO_2$ material had higher proliferation rate as compared to the $0.3Al_2O_3/0.3CeO_2$ material. Despite of having contrasting values, it can be concluded that both 0.3wt% Al_2O_3 /0.5wt% CeO_2 and $0.3Al_2O_3/0.3CeO_2$ materials' rate of cell proliferation clearly indicate that the material is not toxic.

Cell morphology and cell-material interphase study

Both compositions of Al_2O_3/CeO_2 doped 3Y-TZP appears to be biocompatible to human osteoblasts. It provided a nodular surface that supported cell attachment and proliferation. As pore sizes were in average less than 2 μm, cells (approximately 100 μm) did not penetrate into the inner cavity of the material but remain on the material surface. In a study conducted by Garcia et.al [34]., it was found that 3Y-TZP samples compared to Zr-Ti samples adhered better to the cell surfaces. Previous also confirmed that a better osteoblast behaviour is observed on zirconia as compared to titanium [35,36].

Conclusions

The incorporation of Al_2O_3 and CeO_2 dopants had direct influences on the physical and biomechanical properties of the synthesized 3 mol% yttria-stabilized zirconia (3Y-TZP). Generally, the dopants enhanced the tetragonal ZrO_2 stability and the microstructure of 3Y-TZP. The doped 3Y-TZP samples had smaller grain sizes and thus higher hardness values as compared to the undoped samples. The doped 3Y-TZP bioceramic also demonstrated higher cell proliferation than that of undoped samples. Overall, the 3Y-TZP doped with

0.3wt% Al_2O_3 and 0.5wt% CeO_2 holds high potential as an advanced bioceramic for biomedical implant applications.

Acknowledgments

The authors would like to thank the Ministry of Science, Technology and Innovation of Malaysia (MOSTI) for providing the financial support and making this research possible through the e-Science Fund (Grant No. 02-02-03-SF0251). Also, the technical supports provided by UNITEN and UKM to conduct this research are truly appreciated and acknowledged.

Disclosure statement

No potential conflict of interest was reported by the authors.

Funding

This work was supported by the Ministry of Science, Technology and Innovation of Malaysia (MOSTI); [02-02-03-SF0251].

ORCID

Dinesh Ragurajan http://orcid.org/0000-0002-9792-2188

References

[1] Presenda Á, Salvador MD, Peñaranda-Foix FL, et al. Effect of microwave sintering on microstructure and mechanical properties in Y-TZP materials used for dental applications. Ceram Int. 2015;41:7125–7132.
[2] Hoque ME, Daei JMG, Khalid M. Next generation biomimetic bone tissue engineering matrix from poly (L- Lactic Acid) Pla/calcium carbonate composites doped with silver nanoparticles. Curr Anal Chem. 2018;14(3):268–277.
[3] Hoque ME. Robust formulation for the design of tissue engineering scaffolds: A comprehensive study on structural anisotropy, viscoelasticity and degradation of 3D scaffolds fabricated with customized desktop robot based rapid prototyping (DRBRP) system. Mat Sci Eng C. 2017;72:433–443.
[4] Wahab MA, Islam N, Hoque ME, et al. Recent advances in silver nanoparticle containing biopolymer nanocomposites for infectious disease control – A mini review. Curr Anal Chem. 2018;14(6):198–202.
[5] Michael FM, Khalid M, Ratnam CT, et al. Nano hydroxyapatite synthesis using optimized process parameters for load-bearing implant. Bull Mater Sci. 2016;39(1):133–145.
[6] Osman RB, Swain MV. A critical review of dental implant materials with an emphasis on titanium versus zirconia. Materials. 2015;8(8):932–958.
[7] Bruni YL, Garrido LB, Albano MP, et al. Effects of surface treatments on Y-TZP phase stability, microstructure and osteoblast cell response. Ceram Int. 2015;41:14212–14222.
[8] Hoque ME, Jin TW, Mohamed SH. Physical and mechanical characteristics of conventional dental porcelain: effects of exposure environments. Mater Lett. 2015;143:67–70.
[9] Piconi C, Maccauro G. Zirconia as a ceramic biomaterial. Biomater. 1999;20:1–25.
[10] Guazzato M, Albakry M, Ringer S, et al. Strength, fracture toughness and microstructure of a selection of all-ceramic materials. Part II. Zirconia based dental ceramics. Dent Mater. 2004;20:449–456.
[11] McMeeking RM, Evans AG. Mechanics of transformation-toughening in brittle materials. J Am Ceram Soc. 1982;65:242–246.
[12] Chevalier J, Gremillard L. Ceramics for medical applications: a picture for the next 20 years. J Eur Ceram Soc. 2009;29:1245–1255.
[13] Kosmac T, Koljan A. Ageing of dental zirconia ceramics. J Eur Ceram Soc. 2012;32:2613–2622.
[14] Zhang F, Vanmeensel K, Inokoshi M, et al. 3Y-TZP ceramics with improved hydrothermal degradation resistance and fracture toughness. J Eur Ceram Soc. 2014;34:2453–2463.
[15] Durand JC, Jacquot B, Salehi H, et al. Confocal Raman microscopic analysis of the zirconia/feldspathic ceramic interface. Dent Mater. 2012;28(6):661–671.
[16] Zhang TS, Chan SH, Kong LB, et al. Synergetic effect of NiO and SiO_2 on the sintering and properties of 8mol% yttria-stabilized zirconia electrolytes. Electrochim Acta. 2009;54(3):927–934.
[17] Appel CC, Bonanos N, Horsewell A, et al. Ageing behaviour of zirconia stabilised by yttria and manganese oxide. J Mater Sci. 2001;36:4493–4501.
[18] Winnubst L, Ran S, Speets EA, et al. Analysis of reactions during sintering of CuO-doped 3Y-TZP nano-powder composites. J Eur Ceram Soc. 2009;29(12):2549–2557.
[19] Ragurajan D, Golieskardi M, Satgunam M, et al. Advanced 3Y-TZP bioceramic doped with Al_2O_3 and MnO_2 particles potentially for biomedical applications: study on mechanical and degradation properties. J Mater Res Technol. 2018;7(4):432–442.
[20] Su H, Zhang J, Wang H, et al. Effect of solidification path on the microstructure of Al_2O_3–Y_2O_3–zrO_2 ternary oxide eutectic ceramic system. J Eur Ceram Soc. 2012;32(12):3137–3142.
[21] Samodurova A, Kocjan A, Swain MV, et al. The combined effect of alumina and silica co-doping on the ageing resistance of 3Y-TZP bioceramics. Acta Biomater. 2015;11(1):477–487.
[22] Ai Y, Xie X, He W, et al. Microstructure and properties of Al2O3/ZrO2 dental ceramics prepared by two-step microwave sintering. Mater Des. 2015;65:1021–1027.
[23] Michael FM, Khalid M, Walvekar R, et al. Effect of nanofillers on the physico-mechanical properties of load bearing bone implants. Mater Sci Eng C. 2016;67:792–806.
[24] Michael FM, Khalid M, Ratnam CT, et al. Sonosynthesis of nanohydroxyapatite: effects of process parameters. Ceram Int. 2016;42(5):6263–6272.
[25] Santos C, Teixeira LHP, Daguano JKMF, et al. Mechanical properties and cytotoxicity of 3Y-TZP bioceramics reinforced with Al_2O_3 particles. Ceram Int. 2009;35:709–718.
[26] Rejab NA, Azhar AZ, Ratnam MM, et al. The effects of CeO_2 addition on the physical, microstructural

and mechanical properties of yttria stabilized zirconia toughened alumina (ZTA). Int J Refract Metals Hard Mater. 2013;36:162–166.
[27] Niihara K, Morena R, Hasselman DPH. Evaluation of K_{IC} of brittle solids by the indentation method with low crack-to-indent ratios. J Mater Sci Lett. 1982;1:13–16.
[28] Ragurajan D, Satgunam M, Golieskardi M. The effect of cerium oxide addition on the properties and behavior of Y-TZP. Int Sch Res Notices. 2014;2014: Article ID 828197, 5.
[29] Hodgson SNB, Cawley J, Clubley M. The role of Al_2O_3 impurities on the microstructure and properties of Y-TZP. J Mater Process Technol. 1999;92-93:85–90.
[30] Kimura N, Abe S, Hayashi Y, et al. Sintering behavior and anti-degradation property of MOx-doped Y-TZP (M: cu, Mn, Co, Ni, Zn). Sprechsaal. 1989;122(4):341–343.
[31] Ramesh S, Meenaloshini S, Tan CY, et al. Effect of manganese oxide on the sintered properties and low temperature degradation of Y-TZP ceramics. Ceram Int. 2008;34(7):1603–1608.
[32] Strickstrock M, Rothe H, Grohmann S, et al. Influence of surface roughness of dental zirconia implants on their mechanical stability, cell behavior and Osseointegration. BioNanoMat. 2017;18 (1–2):20160013.
[33] Ardlin B. Transformation-toughened zirconia for dental inlays, crowns and bridges: chemical stability and effect of low-temperature aging on flexural strength and surface structure. Dent Mater. 2002;18 (8):590–595.
[34] Garcia EF, Marti JG, Gonzalez CFG, et al. Osteoblastic cell response to spark plasma-sintered zirconia/titanium cermets. Hard Tissues Mater. 2015;29(6):813–823.
[35] Agac O, Gozutok M, Sasmazel HT, et al. Mechanical and biological properties of Al_2O_3 and TiO_2 co-doped zirconia ceramics. Ceram Int. 2017;43(13):10434–10441.
[36] Depprich R, Ommerborn M, Zipprich H. Behavior of osteoblastic cells cultured on titanium and structured zirconia surfaces. Head Face Med. 2008;4(29):1–9.